Available online at www.sciencedirect.com
ScienceDirect
Biochemical and Biophysical Research Communications 349 (2006) 69–78
BBRC
www.elsevier.com/locate/ybbrc

mRNA secondary structure at start AUG codon is a key limiting factor for human protein expression in *Escherichia coli* ☆

Weici Zhang [a], Weihua Xiao [a,b,*], Haiming Wei [a], Jian Zhang [b], Zhigang Tian [a,b,*]

[a] *Hefei National Laboratory for Physical Sciences at Microscale and School of Life Sciences, University of Science and Technology of China, Hefei, Anhui 230027, China*

[b] *School of Pharmaceutical Sciences, Shandong University, Jinan, Shandong 250012, China*

Received 14 July 2006
Available online 11 August 2006

Abstract

Codon usage and thermodynamic optimization of the 5′-end of mRNA have been applied to improve the efficiency of human protein production in *Escherichia coli*. However, high level expression of human protein in *E. coli* is still a challenge that virtually depends upon each individual target genes. Using human interleukin 10 (huIL-10) and interferon α (huIFN-α) coding sequences, we systematically analyzed the influence of several major factors on expression of human protein in *E. coli*. The results from huIL-10 and reinforced by huIFN-α showed that exposing AUG initiator codon from base-paired structure within mRNA itself significantly improved the translation of target protein, which resulted in a 10-fold higher protein expression than the wild-type genes. It was also noted that translation process was not affected by the retained short-range stem–loop structure at Shine–Dalgarno (SD) sequences. On the other hand, codon-optimized constructs of huIL-10 showed unimproved levels of protein expression, on the contrary, led to a remarkable RNA degradation. Our study demonstrates that exposure of AUG initiator codon from long-range intra-strand secondary structure at 5′-end of mRNA may be used as a general strategy for human protein production in *E. coli*.

Keywords: Codon optimization; RNA stability; Start codon; Secondary structure; Interleukin 10; *E. coli*

Production of human proteins using prokaryotic expression system becomes a much higher demand for functional and structural analysis of numerous gene products, as well as for pharmaceutical productions because its advantages in low-cost and high yield over mammalian system. The regulation of gene expression in *Escherichia coli* has been relatively well understood, and commercial available expression vectors have also provided a wide range of choices, however, high level expression of human proteins in *E. coli* is still a challenge that virtually depends upon each individual target genes [1,2]. A variety of factors that significant influence protein expression in *E. coli* have been identified, among which, codon usage, RNA secondary structures and mRNA stability have been the major concerns [3–5].

Human IL-10 (huIL-10) is a pivotal cytokine that predominantly exerts immunosuppress activity, and plays an important role in negative control of autoimmunity. HuIL-10 cDNA encodes a 160 amino acid mature peptide that contains all the major rare codons for *E. coli*, includes AGA and AGG for arginine, AUA for isoleucine, CUA for leucine, and CCC for proline. As previously reported, wild-type huIL-10 cDNA is poorly expressed in *E. coli* [6]. In the present study, using the coding sequence of huIL-10 and huIFN-α as the examples, we have systematically tested the influences of the major elements on human protein expression in *E. coli*. The results from the expression of huIL-10 and reinforced by huIFN-α showed that RNA secondary structure at initiator AUG

☆ *Abbreviations:* huIL-10, human interleukin 10; huIFN-α, human interferon α; SD, Shine–Dalgarno; LB, Luria–Bertani; RBS, ribosome-binding site.

* Corresponding authors.
E-mail addresses: xiaow@ustc.edu.cn (W. Xiao), tzg@ustc.edu.cn (Z. Tian).

0006-291X/$ - see front matter © 2006 Elsevier Inc. All rights reserved.
doi:10.1016/j.bbrc.2006.07.209

codon is the key limiting factor for high-level expression of huIL-10 in *E. coli*. Thus, our study supplies a novel convenience strategy for improving human protein expression in *E. coli*.

Materials and methods

Reagents. Oligonucleotides and pCR–TOPO derived vector was purchased from Invitrogene (Carlsbad, CA). Restriction and modification enzymes were purchased from New England Biolabs (Beverly, MA). *E. coli* expression strain BL21 (DE3) Gold, *Pfu*, and Tag DNA Polymerase were purchased from Strategen (Cedar Creek, TX). QIAquick Gel extraction Kit, QIAprep Spin Miniprep Kit, QIAquick PCR purification Kit, and RNeasy Mini Kit were purchased from QIAGEN (Valencia, CA). All growth medium were purchased from Difco (UK) and all the chemical reagents were from Sigma–Aldrich. Sequencing was performed according to a dideoxy terminator protocol.

Plasmid construction. The cDNAs containing the coding sequence for mature peptide of human IL-10 and human interferon-α were amplified by RT-PCR from total RNA isolated from human bone marrow (Clonetech) and cloned into pCR-TOPO derived vector according to manufacture's instructions. The primer sets used for cloning of huIL-10 cDNA were upstream primer: 5′-ATG AGC CCA GGC CAG GGC AC-3′, downstream primer: 5-TTA TTA GTT TCG TAT CTT CAT TGT C-3′, for cloning of huIFN-α were: upstream primer: 5′-ATGTGTGATCTG CCTCAAACCCACA-3′ and downstream primer: 5′-TTATGTCATG GTCATAGCAGAAAC-3′. On both primer sets for huIL-10 and huIFN-α, additional start codon ATG and the stop codon TAA were added to the 5′-end of the upstream and downstream primers respectively and indicated as underlines. The resulted clones were designated as pCR-huIL10-wt and pCR-IFNα-wt for huIL-10 and huIFNα coding sequences, respectively. pCR-huIL10-wt was then used as the backbone for generating the pCR-huIL10-ILRP by introducing the silent mutations into the major rear codons, including AGA and AGG (Arg), which are the rarest codons in *E. coli*, AUA (Ile), CUA (Leu), and CCC (Pro). pCR-huIL10-5′, pCR-huIL10-3′, pCR-huIL10-5′3′, and pCR-huIL10-ILRP-5′, pCR-huIL10-ILRP-3′, and pCR-huIL10-ILRP-5′3′ which containing the either or both of 5′-end and 3′-end modifications for reducing the stabilities of RNA secondary structures were also created by PCR-based site-directed mutagenesis based on the pCR-huIL10-wt and pCR-huIL10-ILRP. The pCR-huIL10-TM contains a synthesized sequence that code for mature huIL-10 peptide by altering all of the codons toward to *E. coli* favorite ones using Online Codon Maximizer program from MCLAB at: http://www.mclab.com/toolbox/codonMaximization.html. The pCR-IFNα-wt5′ that contains 5′-end modified coding sequence for huIFN-α was also created using the pCR-IFNα-wt as the template. All the recombinants that created in this study were verified by DNA sequencing.

Growth and IPTG inductions of transformed BL21 (DE3). To induce the expression of the recombinant protein, 1 mM/ml of IPTG was added and cultured for 3 h. The uninduced samples were cultured under the same conditions as induced except without the additional IPTG. By the end of induction, the bacterial were harvested by centrifugation at 4000*g* for 10 min at 4 °C and either freeze at −80 °C or preceded immediately for further use.

Western blot. After electrophoresis the proteins were transferred onto Immobilon P membranes (Millipore) by Trans-Blot SD Semi-Dry Transfer Cell (Bio-Rad) according to manufacturer's guides. The membranes were blocked with 5% non-fat dried milk/TBST (137 mM NaCl, 15 mM Tris–HCl (pH 7.6), and 0.1% Tween 20) for overnight at 4 °C, then incubated for 1 h at room temperature with monoclonal anti-huIL-10 antibody (Santa Cruz Biotechnology, CA) for 2 h at 4 °C. After four 5-min washes in TBST, the membranes were incubated in 2.5% non-fat dried milk/TBST with goat anti-mouse HRP conjugate antibody (Amersherm Biosciences KK) with 1:50,000 dilution for 40 min at room temperature. Following four washes with TBST, the signal was detected using Super-Signal Chemiluminescent Substrate (Pierce Chemical Co., Rockford, IL) and exposed with X-ray film.

RNA secondary structure prediction. RNA structures were analyzed using the algorithm of favorite thermodynamic by Vienna RNA Secondary Structure Prediction program on the web at http://rna.tbi.univie.ac.at/cgi-bin/RNAfold.cgi.

Isolation of total RNA from E. coli and RT-PCR. Total RNA was extracted from previously collected bacterial cells using TRIzol (Invitrogen, Carlsbad, CA) according to the manufacturer's instructions. After precipitation, the total RNA was resuspended in RNase-free water and analyzed by UV spectrometer for both quantity and quality assay. The corresponding tRNAs were visualized by ethidium bromide staining after electrophoresis on a 1% agarose/formaldehyde gel. To eliminate the possible DNA contamination, the total bacterial RNA was first treated with RNase free DNase I (MBI Fermentas, hanover, MD) at 1 U/μg total RNA for 30 min at 37 °C and purified with RNeasy Mini Kit (Qiagen) according to the manufacturer's instructions. Then 2 μg of RNA was subjected for reverse transcription using M-MLV Reverse Transcriptase (Invitrogen, Carlsbad, CA) and random hexamer primers according to the manufacturer's instructions. cDNAs were then amplified with the corresponding gene-specific primer sets by PCR for 30 cycles under the condition of 30 s at 94 °C, 1 min at 58 °C, and 1 min at 72 °C. The PCR products were analyzed on a 1.5% agarose gels containing 0.5 μg/ml ethidium bromide. If the PCR products were used for cloning, then the corresponding bands were excised from the agarose gel and recovered by QIAquick Gel extraction Kit.

Results

Optimizations of codon bias had no effect on huIL-10 mRNA translation in E. coli

To evaluate the influence of codon bias for huIL-10 expression in *E. coli*, pCR-huIL10-CodonMax and pCR-huIL10-ILRP plasmids were constructed as described in methods. After induced by 1 mM IPTG, the protein expression levels were detected by Coomassie blue staining and Western Blot with anti-huIL-10 antibody. Unexpectedly, the expression of target protein showed no apparent change in comparison with pCR-huIL10-wt clone (Figs. 1A and B). Because ribosomes can bind to the 5′-end of the growing mRNA to initiate translation before synthesis of the mRNA is completed, and the steady-state transcription level reflects the results of both RNA synthesis and degradation in prokaryocytes, we further examined the transcription status in these expression clones by RT-PCR. The results showed that no significant differece was observed in mRNA levels between pCR-huIL10-wt and pCR-huIL10-ILRP (Fig. 1C). Surprisingly, a less mRNA transcription level was obtained in pCR-huIL10-CodonMax. Above evidence implicates that the inhibitory factor in huIL-10 expression is most likely due to the mRNA secondary structure, but not codon usage.

Exposure of AUG start codon from base-paired mRNA structure improved the huIL-10 protein expression

By inspecting the sequences of IL10-wt with Vienna online program using thermodynamic algorithm in search for the most energetically favored structure, a possible long-range secondary structure spanning at ribosome-

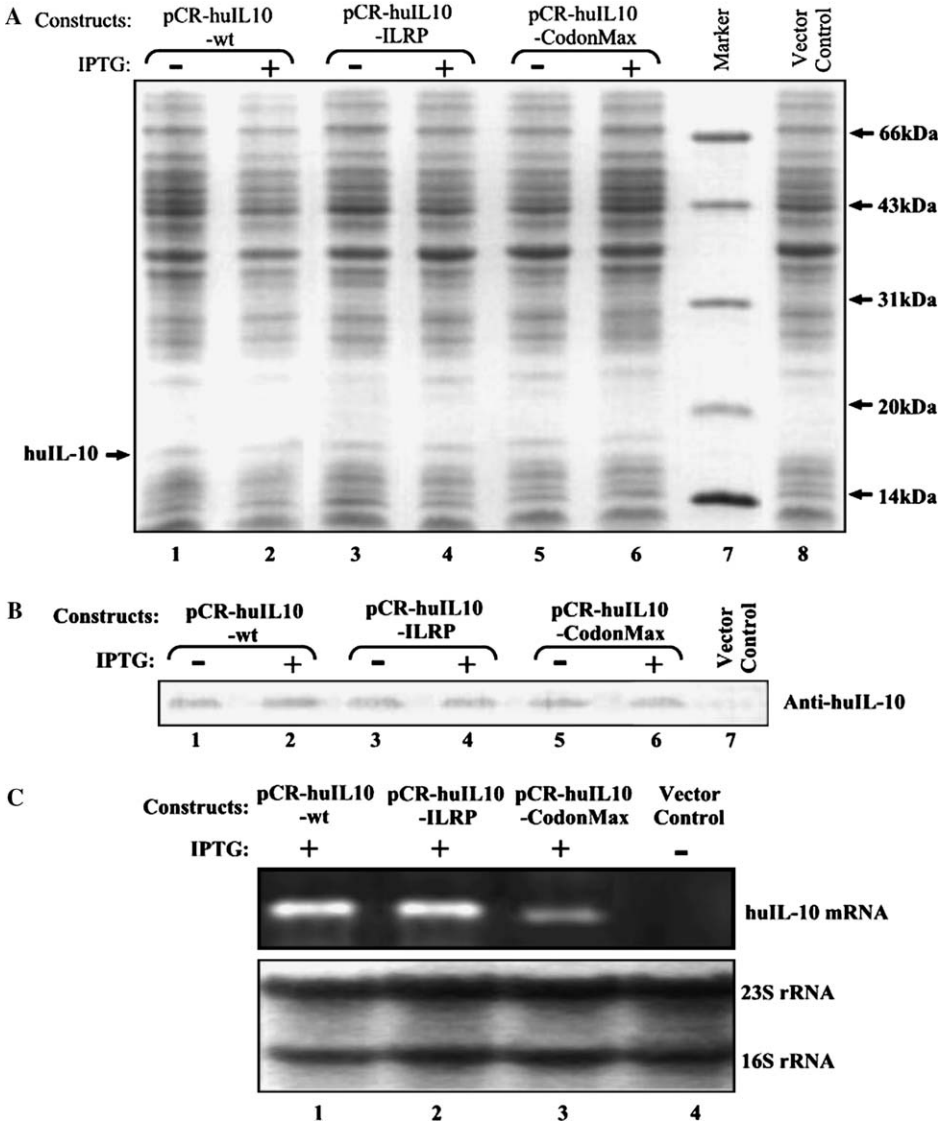

Fig. 1. Optimizations of codon bias had no effect on huIL-10 protein expression in *E. coli*. The protein expression pattern from pCR-huIL10-wt, pCR-huIL10-ILRP, and pCR-huIL10-CodonMax transformed BL21 (DE3) strains were examined by reduced SDS–PAGE (A), or Western blot (B) with monoclonal anti-huIL-10 antibody. The mRNA levels were detected by RT-PCR (C) with gene-specific primers after cDNA synthesis from total RNA isolated from corresponding expression strains as indicated. The quality and quantity of total RNA used for RT-PCR were evaluated by running 5 μg total RNA on a formaldehyde agarose gel and visualized by ethidium bromide staining (C). The BL21 strain transformed with empty vector was used as vector controls as indicated in all the experiments.

binding site (RBS), translation initiator AUG and the first seven codons was predicted (Fig. 2A). The corresponding pilot of free energies for each nucleotide and the overall free energy were calculated and indicated in Fig. 2B. To expose start AUG codon from intra-strand structure, six silent mutations were introduced into the first few codons of huIL10-wt (Fig. 2E) and huIL10-ILRP, in which the single long-range secondary structure was separated into two small stem–loops, one locating at SD region and the second locating at the first seven codons down stream of AUG initiator with free energy of −3.8 and −4.7 kcal/mol, respectively (Figs. 2C and D). The data showed that AUG initiator site-exposed clones had significantly higher translation efficiency than pCR-huIL10-wt clone (Fig. 3A). Photometry intensities of each corresponding bands were then measured by gel scanning (Fig. 3B), showing that 11-fold increase accounts for 20% of total host cellular proteins were achieved from both pCR-huIL10-wt5′ and pCR-huIL10-ILRP5′. The specificity of the target product was further confirmed by Western blot with monoclonal anti-human IL-10 antibody (Fig. 3C). In contrast with the protein level, the specific mRNAs from those clones were also tested later and showed a equal expression level (Fig. 5B), indicating that modifications on the translation initiator sequence effectively improve the translation and have no negative influence on the transcription process and the stability of the mRNA.

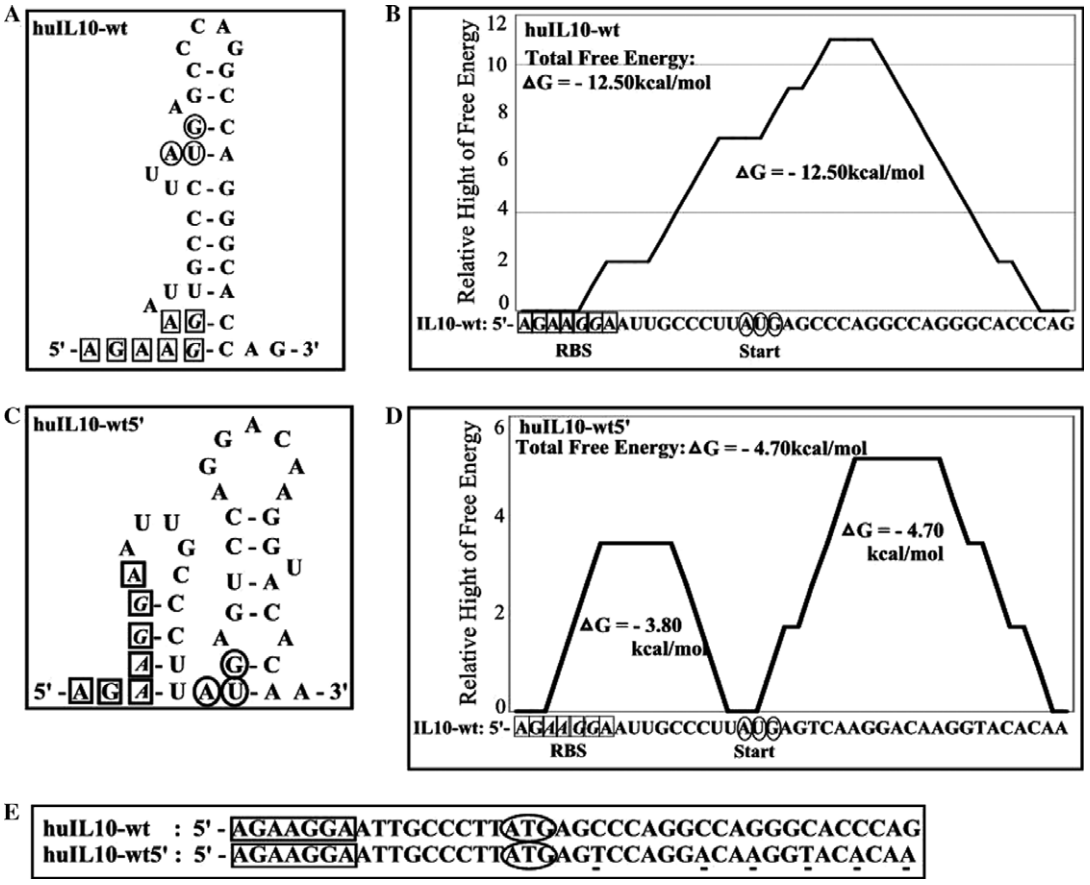

Fig. 2. Illustration of RNA secondary structures predicted at 5′-end of huIL10-wt and pCR-huIL10-wt5′. The theoretical Δ*G* values of RNA secondary structures at 5′-end of pCR-huIL10-wt (A) and pCR-huIL10-wt5′ (C) were calculated by Vienna RNA Secondary Structure Prediction program (http://rna.tbi.univie.ac.at/cgi-bin/RNAfold.cgi) with thermodynamic algorithm and illustrated. The energy pilot for each nucleotides that participated in the secondary structures were also calculated and illustrated with line graph in (B) for pCR-huIL10-wt and in (D) for pCR-huIL10-wt5′. The initiator AUG codon and SD sequence were indicated with circles and boxes, respectively, and the nucleotides that forming base-pair in the secondary structures within SD region were indicated with italic letters. The sequence alignment with pCR-huIL10-wt and pCR-huIL10-wt5′ was presented in (E), where the nucleotides with underline indicated the substitutions with synonymous codons.

Reduction in the stability of RNA structure at 3′-end of mRNA led to much lower production of huIL-10 protein

We also explored the roles of the secondary structure at 3′-end for the expression of huIL-10 in the *E. coli*. The analysis with Vienna online program showed that a long-range intra-strand RNA structure at just few nucleotides before the terminate TAA codon was predicted total free energy of −7.0 kcal/mol (Fig. 4). To investigate the effect of 3′-end of mRNA stability on the translation of huIL-10 mRNA, eleven silent mutations were introduced by site-directed mutagenesis. The number of nucleotides spanned in the intra-strand structure was reduced from 40 nucleotides to 20 nucleotides and the number base-paired nucleotides were reduced from 10 to 7, in comparison between pCR-huIL10-wt and pCR-huIL10-wt3′, and the total free energy was increased from −7.0 to −3.3 kcal/mol. In additional, the same modifications were also applied on pCR-huIL10-ILRP, pCR-huIL10-wt5′, and pCR-huIL10-ILRP5′. The mRNA and protein expression levels were detected in all constructs containing 3′-end modifications. More surprisingly, the remarkable decrease was observed in both mRNA (Fig. 5B) and protein (Fig. 5A) expression levels, suggesting that the reduced stability of RNA structure at 3′-end exerts a significant negative effect on protein expression.

Exposure of initiator AUG in huIFN-α mRNA intra-strand structure also greatly improved the translation

The huIFN-α cDNA was cloned and expressed in the same expression system as used for huIL-10. The expression production of the wild-type huIFN-α genes was only 3.6% of total host proteins A and C) (Fig. 7B). Analyzing the 5′-end of the sequence including RBS and 54 nt downstream of start codon AUG, two stem–loops with total free energy of −19.38 kcal/mol were predicted (Figs. 6A and C), although the SD site was totally exposed in single strand. One of the stem–loop was a relative long-range intra-strand structure with 44 nt and 12 base-paired located between RBS region and 10 codons upstream initiator AUG, this structure was speculated the blockade element for gene translation

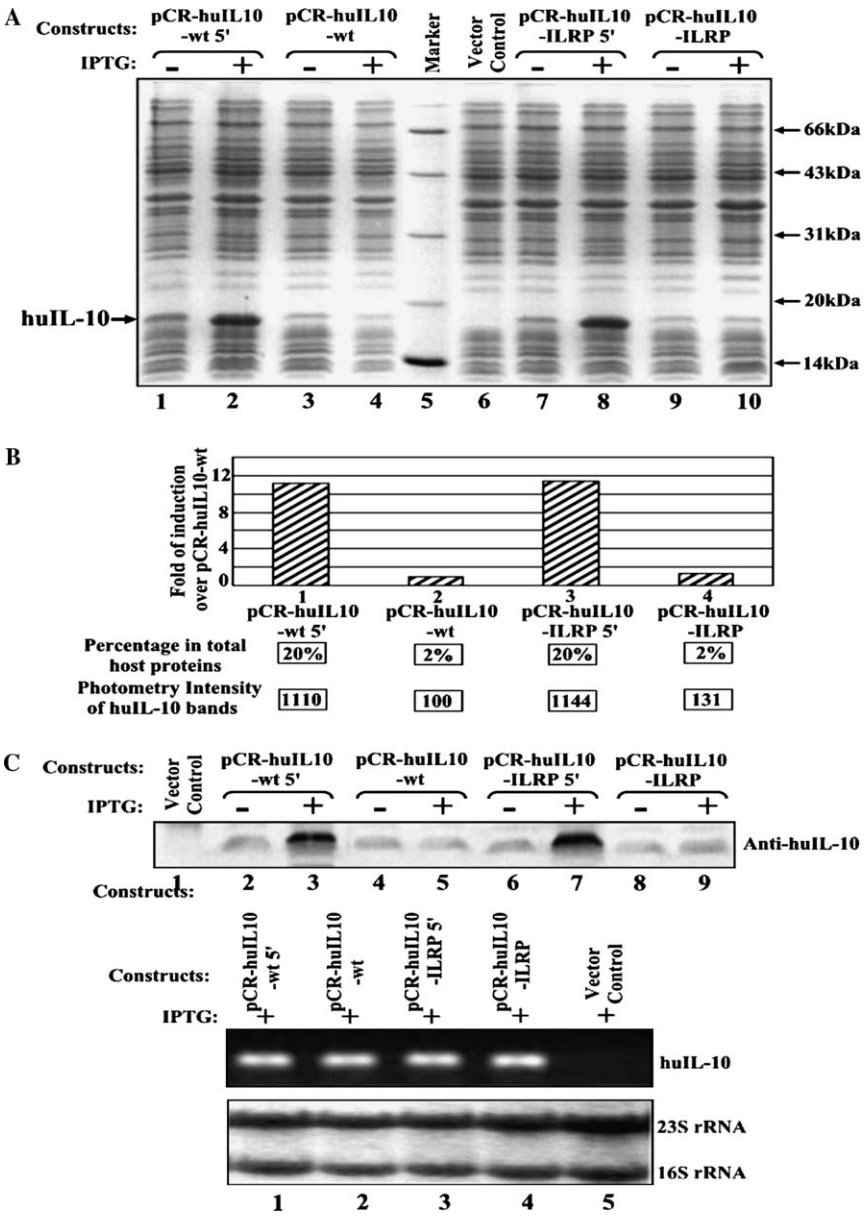

Fig. 3. Exposure the initiator AUG codon from intrastrand structure increased the target protein production. The protein expression patterns from transformed BL21 (DE3) strains with various constructs as indicated were detected with SDS–PAGE (A) and Western blot (C). The relative photometry intensity for the total cellular proteins and the bands corresponding to the target protein in IPTG induced samples (A, lanes 2, 4, 8, and 10) were measured by gel scanning and the percentage of target proteins in total host soluble proteins are calculated and indicated in (B). The bar graph in (B) represented the relative fold according to the measurements of photometry intensity from corresponding bands and compared to the pCR-huIL10-wt.

efficiency. To expose the initiator AUG codon, total 18 silent mutations were introduced into huIFN-α (Fig. 6E). This modification resulted in a fully exposure of AUG start codon and a four-base-paired stem loop formed at SD region with free energy of −4 kcal/mol and a long-range secondary structure downstream of the AUG start codon (Figs. 6B and D). The production of target protein in huIFNα-wt5′ was 12-fold higher than huIFNα-wt clone and enhanced to 20% of total host proteins. The data further confirmed that altering local secondary structure to just expose the initiator AUG can effectively improve the translation, in despite of the total free energy had not sharply increased.

Discussion

In this report, we describe the correlation between translation efficiency and RNA secondary structure at initiator AUG site, which serves as a strongly negative regulator for human protein synthesis in *E. coli*. Silent mutation into the 5′-end of mRNA based on the analysis of RNA secondary structure in order to just expose the start codon AUG were confirmed to effectively promote the translation efficiency in our established expression systems. It should be noted that codon bias has been considered as the most important factor that often causes early termination of

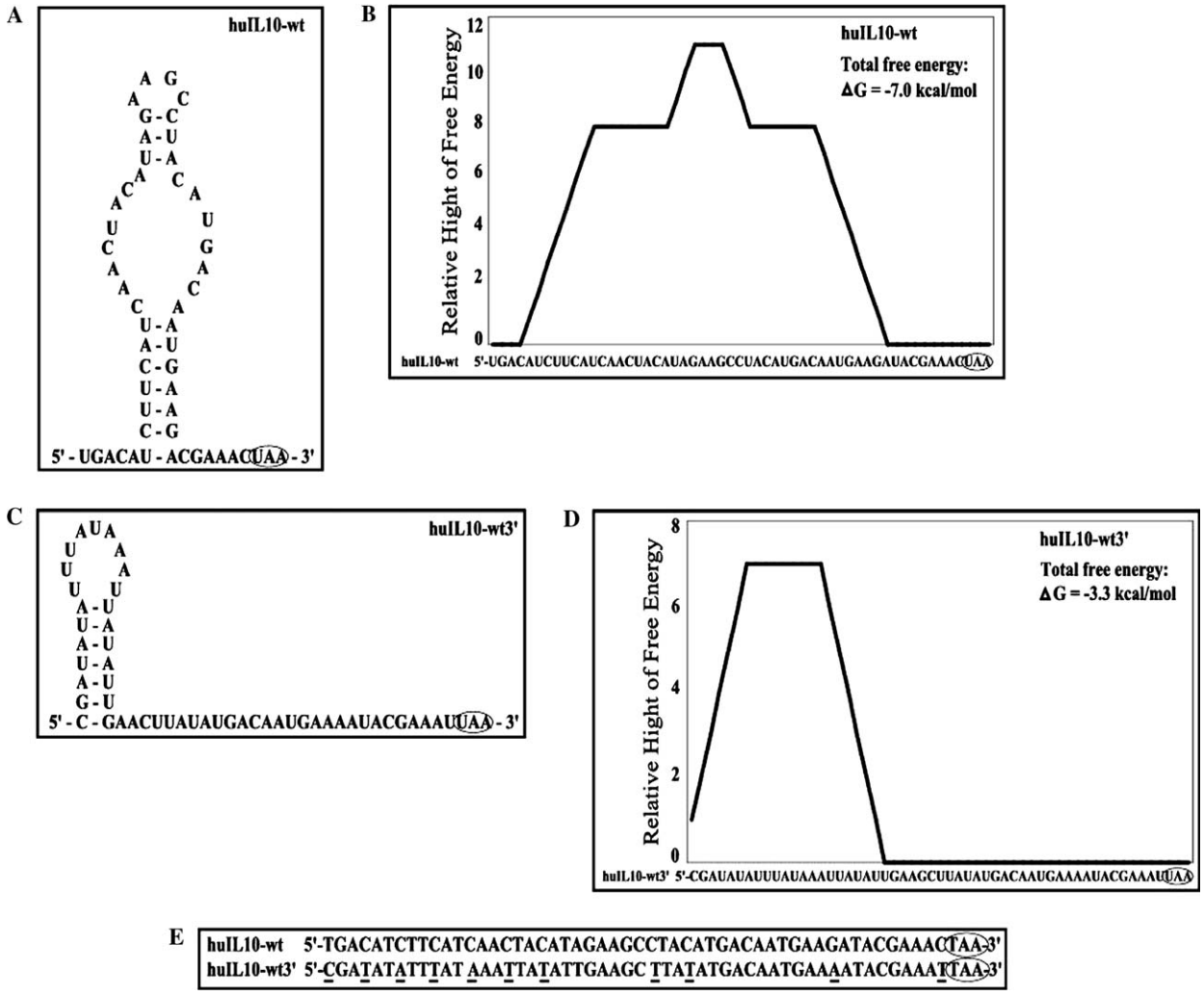

Fig. 4. Illustration of RNA secondary structures predicted at 3′-end of pCR-huIL10-wt and pCR-huIL10-wt3′. The theoretical Δ*G* values of RNA secondary structures at 3′-end of pCR-huIL10-wt (A) and pCR-huIL10-wt3′ (C) were calculated by Vienna Prediction program with thermodynamic algorithm and illustrated. The energy pilot for each nucleotides that participate in the secondary structures were also calculated and illustrated with line graph in (B) for pCR-huIL10-wt and in (D) for pCR-huIL10-wt3′. The terminator TAA codon was indicated with circles and boxes, respectively. The sequence alignment with pCR-huIL10-wt and pCR-huIL10-wt3′ was presented in (E) where the nucleotides with underline indicated the substitutions with synonymous codons.

translation for non-host protein synthesis [7–10]. One of commonly employed strategies is substitution of the rare codons to the host preferred ones [11–13]. In our study, we functionally analyzed the rare codons of human IL-10 gene and exploited two different approaches to optimize the rare codons, but no significant increase in huIL-10 protein expression were detected in both codon optimized constructs (pCR-huIL10-ILRP and pCR-huIL10-CodonMax) (Figs. 1A and B). This result was consistent with the previously report, which showed that codon optimization led to significantly lower expression compared to the wild-type fungal cutinase gene [14]. Considering codon optimization could result in the significant changes on RNA secondary structure and the rate of RNA degradation, we further analyzed the transcription levels in those clones and predicted the RNA secondary structure at 5′-end or 3′-end. Expression levels of IL-10 mRNA were unaltered between pCR-huIL10-wt and pCR-huIL10-ILRP transforms, but the significantly lower levels of IL-10 transcript was detected in pCR-huIL10-CodonMax clones (Fig. 1C), suggesting that codon optimizations did not improve huIL-10 protein expression in *E. coli*. In addition, it had been predicted that total free energy of the long-range structure between RBS and 5′ coding sequence was decreased to −13.32 kcal/mol but the intra-strand structure located at AUG codon had not altered apparently in pCR-huIL10-CodonMax clone. Meanwhile, the total free energy at the 3′ end of mRNA was increased from −7.0 to −4.9 kcal/mol (data not shown), implying that unstable RNA secondary structure at 3′-end eventually caused mRNA degradation. These results highlight the important roles of 5′- or 3′-end secondary structure for non-host protein expression in *E. coli*.

Secondary structures at RBS have been found to closely correlate with the translation efficiency, where three ele-

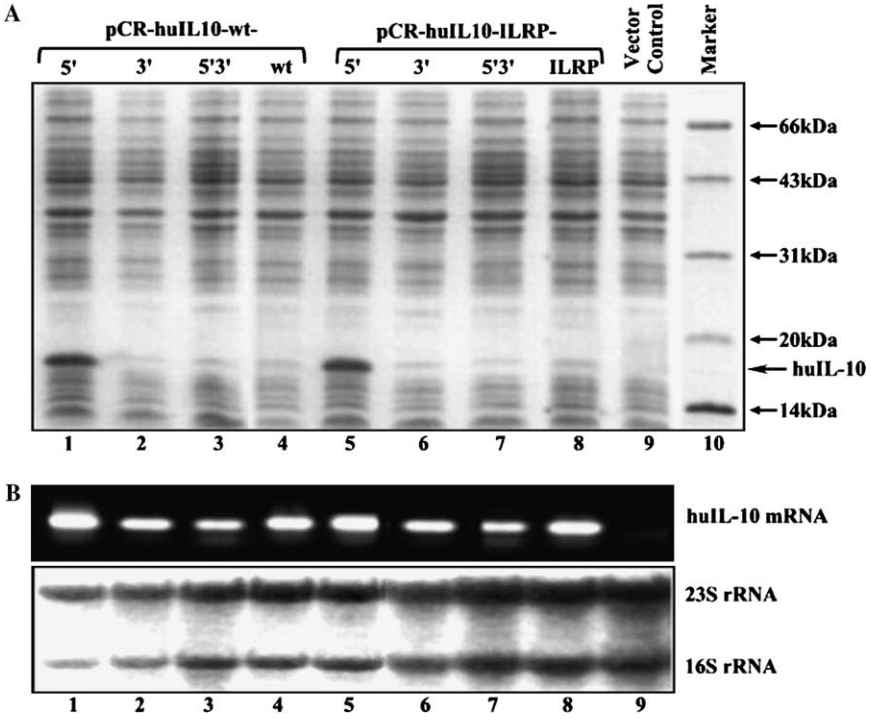

Fig. 5. Reduction in the stability of RNA secondary structure at 3′-end of huIL-10 mRNA led to rapid RNA degradation. The protein expression pattern and the level of corresponding transcripts from various constructs as indicated were evaluated by SDS–PAGE and RT-PCR with the same protocol as described as in Fig. 1.

ments including SD sequence, start codon AUG and the space between SD and start codon AUG are considered as the most important factors [15,16]. Long-range RNA secondary structures at the RBS region have been demonstrated the inhibitory element for translation initiation [17–19]. However, recent studies have demonstrated that the short stem–loops at the front or downstream region of initiator ATG codon could either enhance or reduce the protein productions [20–23], while another study found that the short-range structure at 5′-end of mRNA has no effect to the translation efficiency unless its free energy is less than −6.0 kcal/mol [24]. In our current study, the alternations on pCR-huIL10-wt5′ and pCR-huIL10-ILRP5′ have increased overall free energy of the long-range structure from −12.5 to −4.7 kcal/mol (Fig. 2D), the translation initiator site AUG also exposed from the long-range secondary structure consequently. Although the base-paired structure located at the SD site was more stable and the paired bases were increase from 2 nucleotides to 4 nucleotides in pCR-huIL10-wt5′ clone (Figs. 2A and C), the expression of target protein was significantly higher than the wild-type pCR-huIL10-wt (Fig. 3B). Related to the role of secondary structure at AUG site, Birgit Klinkert and his colleague have found that a secondary RNA structure encompassing the AUG initiation codon within a double-stranded region blocks the translation of psbD mRNA and serves as a negative regulatory determinant for the synthesis of the D2 protein in *chlamydomonas* [25]. Similarly, our results have implicated that exposing and reducing the stability of secondary structure at AUG site could possesses an extended advantage for improving the translation efficiency in *E. coli* and also revealed that if the overall free energy of the secondary structure at RBS region is less than −6.0 kcal/mol, it has no inhibitory effects on the translational efficiency. Furthermore, as the result of silent mutation for the initiator AUG codon exposure, there is a conversion from G/C-rich to A/U-rich initiation region, which has been described previously that optimization of the A/U-content of codons immediately downstream of the initiation codon improve the heterologous gene expression in *E. coli* [26,27]. Results obtained from the expression of human interferon-α (huIFN-α) using the same expression system further confirmed that changing the local RNA secondary structure at initiator AUG codon could effectively stimulate the translation of target gene (Fig. 7).

Additionally, bioinformatic inspection of the 3′-end of huIL-10 mRNA in pCR-huIL10-CodonMax clone shows a decreased thermodynamic stability, which appears the major cause for much lower transcription of huIL-10 mRNA than wild-type. To confirm our speculation, similar unstable secondary structure as pCR-huIL10-CodonMax was obtained by introducing eleven silent mutations into 3′-end of huIL-10 gene. Moreover, those point mutations were also introduced into pCR-huIL-10-wt5′ and pCR-huIL10-ILRP5′, the high-level expression of huIL-10 protein clones, which will provide an answer to the question whether such unstable secondary structure at 3′-end contributes to the poor mRNA transcription. Besides the

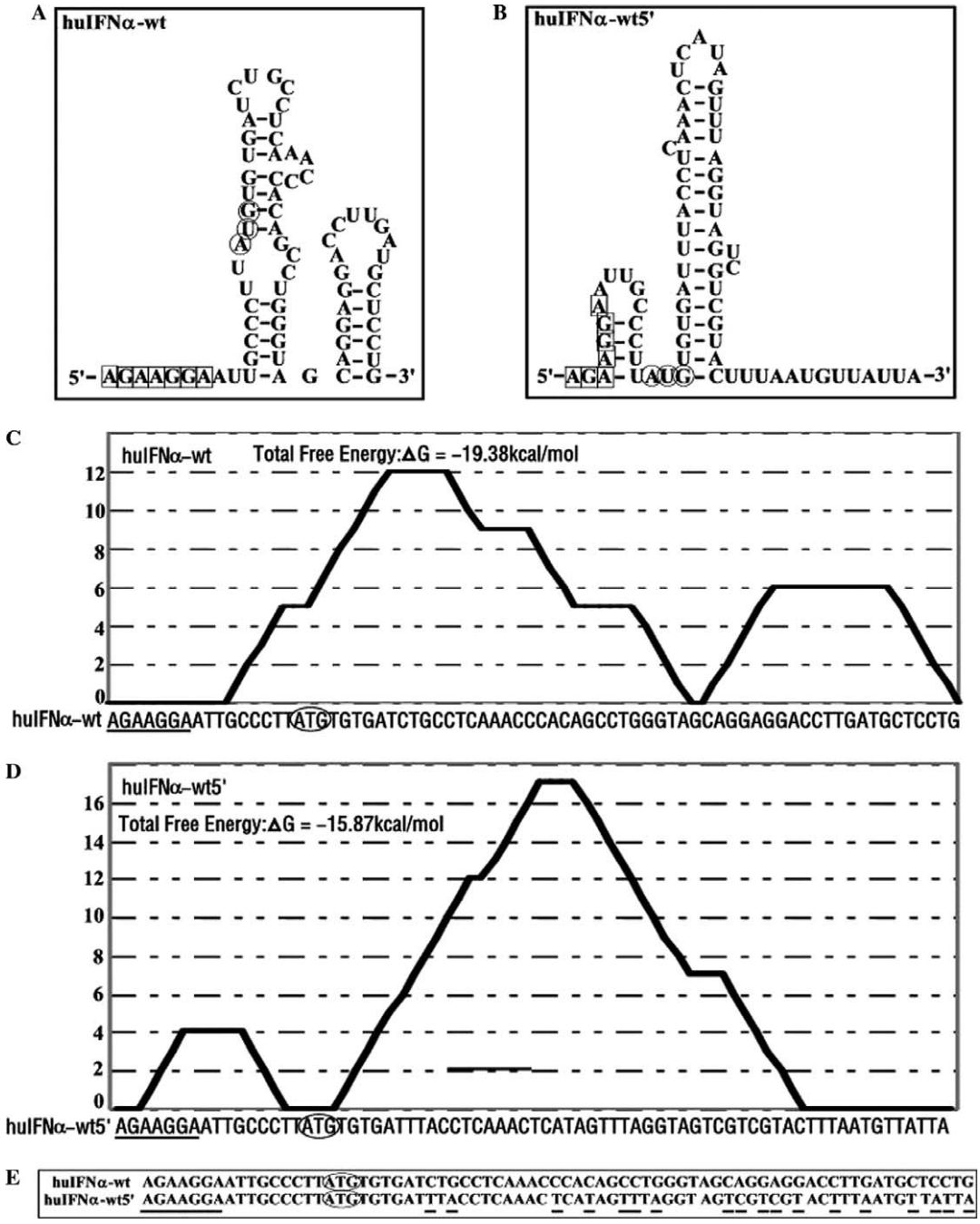

Fig. 6. Illustration of RNA secondary structure predicted at 5′-end of huIFNα-wt. The theoretical ΔG values of RNA secondary structures at 5′-end of huIFNα-wt (A) and huIFNα-wt5′ (B) were calculated by Vienna Prediction program and illustrated. The initiator AUG codon and SD sequence were indicated with circles and boxes respectively and the nucleotides that forming base-pair in the secondary structures within SD region were indicated with italic letters. The sequence alignment with huIFNα-wt and huIFNα-wt5′ was presented in (C), where the nucleotides with underline indicated the substitutions were made with synonymous codons.

decreased transcription of huIL-10 mRNA, the suppression of huIL-10 synthesis was also observed in pCR-huIL10-wt5′3′ and pCR-huIL10-ILRP5′3′ clones and the lack of protein synthesis was found in pCR-huIL10-wt3′, pCR-huIL10-ILRP3′ clones (Fig. 5). Previous studies indicated that stem–loop secondary structures in 3′ UTR of prokaryotic message apparently protect against degradation by the exonucleases RNase II and PNPase [28–30]. All these accumulated data implied that long-range secondary structure of 3′-end mRNA is a critical factor to maintain the thermodynamic stability, on the contrary, such long-range secondary structure at 5′-end, particularly at AUG start site, remarkably suppressed the translation of non-host protein in *E. coli*.

In conclusion, different from the mammalian cells, the transcription and translation are tightly coupled in

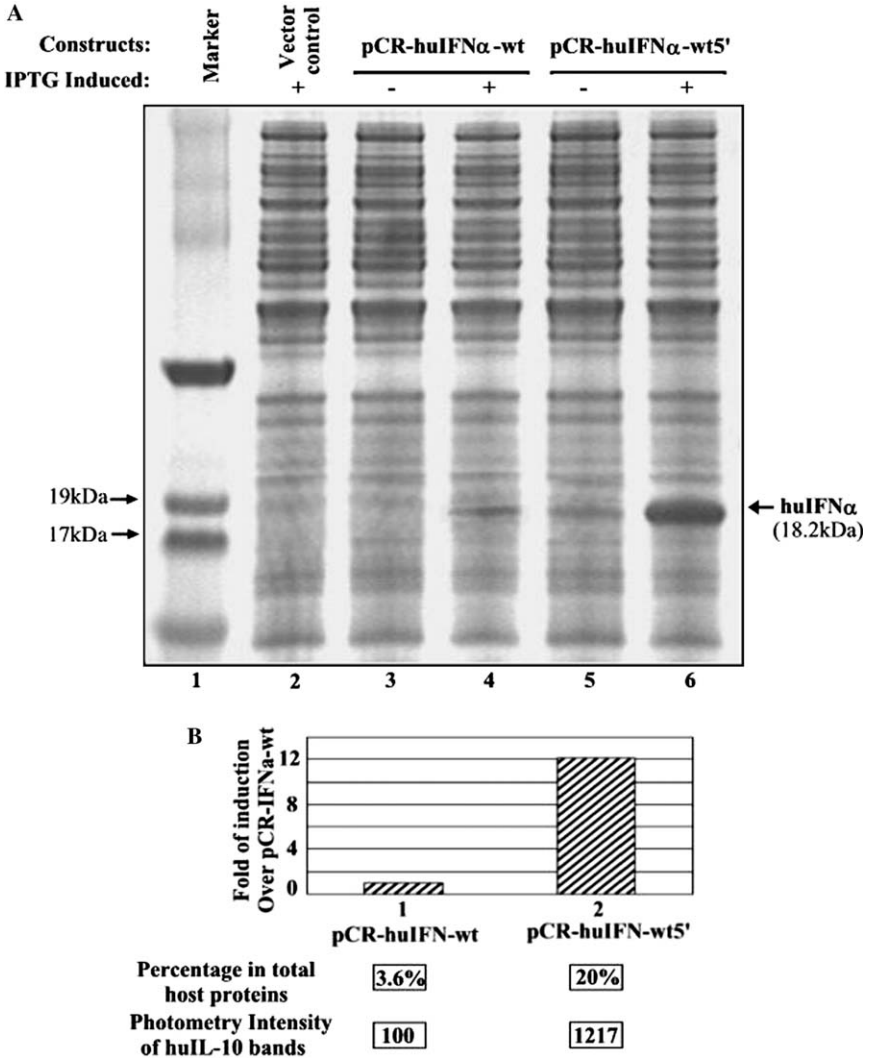

Fig. 7. Exposure of AUG start codon from base-paired mRNA structure improved protein production of recombinant huIFN-α in *E. coli*. The protein expression patterns from transformed BL21 (DE3) strains with pCR-huIFNα-wt and pCR-huIFNα-wt5′ are detected with the SDS–PAGE (A) and the relative photometry intensity for the total cellular proteins and the target bands in IPTG induced samples (A, lanes 4 and 6) were measured by gel scanning as same as in Fig. 1 and indicated in (B). The bar graph in (B) represented the relative fold inductions according to the photometry intensity from corresponding bands as indicated and compared to the photometry intensity of the target band in pCR-huIFNα-wt.

E. coli. RNA folding seems formed only partially but not necessarily in full length, particularly for 5′-end where both transcription and translation initiate. Thus, searching only a partial of 5′ sequences including 5′-UTR and 20–50 nt downstream of initial codon AUG for secondary structure analysis instead of a full length coding sequence might be more reliable to reflect the *in vivo* situation. Furthermore, the strategy of optimization of a partial RNA secondary structure at initiator AUG site that we have used in this study can be suggestive as a general approach for the expression of high-level homologous protein in *E. coli*.

Acknowledgments

This work was supported by Outstanding Young Scientist Award and Key Project of Natural Science Foundation of China (#30125038, #30528020) and Key Basic Science Program by Ministry of Science and Technology of China (#2003CB515501).

References

[1] P. Balbas, Understanding the art of producing protein and nonprotein molecules in *Escherichia coli*, Mol. Biotechnol. 19 (2001) 251–267.
[2] G. Hannig, S.C. Makrides, Strategies for optimizing heterologous protein expression in *Escherichia coli*, Trends Biotechnol. 16 (1998) 54–60.
[3] P.J. Schlax, D.J. Worhunsky, Translational repression mechanisms in prokaryotes, Mol. Microbiol. 48 (2003) 1157–1169.
[4] J.F. Kane, Effects of rare codon clusters on high-level expression of heterologous proteins in *Escherichia coli*, Curr. Opin. Biotechnol. 6 (1995) 494–500.
[5] S. Jana, J.K. Deb, Strategies for efficient production of heterologous proteins in *Escherichia coli*, Appl. Microbiol. Biotechnol. 67 (2005) 289–298.

[6] L.R. Ptitsyn, I.B. Al'tman, M.V. Gurov, Expression of synthetic human interleukin-10 gene and its mutant variants in *Escherichia coli* cells, Bioorg. Khim. 24 (1998) 48–57.
[7] S. Das, S. Paul, S. Chatterjee, C. Dutta, Codon and amino Acid usage in two major human pathogens of genus bartonella—optimization between replicational–transcriptional selection, translational control and cost minimization, DNA Res. 12 (2005) 91–102.
[8] V. Ramachandiran, G. Kramer, B. Hardesty, Expression of different coding sequences in cell-free bacterial and eukaryotic systems indicates translational pausing on *Escherichia coli* ribosomes, FEBS Lett. 482 (2000) 185–188.
[9] D.E. McNulty, B.A. Claffee, M.J. Huddleston, M.L. Porter, K.M. Cavnar, J.F. Kane, Mistranslational errors associated with the rare arginine codon CGG in *Escherichia coli*, Protein Expr. Purif. 27 (2003) 365–374.
[10] E. Goldman, A.H. Rosenberg, G. Zubay, F.W. Studier, Consecutive low-usage leucine codons block translation only when near the 5′ end of a message in *Escherichia coli*, J. Mol. Biol. 245 (1995) 467–473.
[11] F.F. Hamdan, A. Mousa, P. Ribeiro, Codon optimization improves heterologous expression of a *Schistosoma mansoni* cDNA in HEK293 cells, Parasitol Res. 88 (2002) 583–586.
[12] T. Kleber-Janke, W.M. Becker, Use of modified BL21(DE3) *Escherichia coli* cells for high-level expression of recombinant peanut allergens affected by poor codon usage, Protein Expr. Purif. 19 (2000) 419–424.
[13] A. Li, Z. Kato, H. Ohnishi, K. Hashimoto, E. Matsukuma, K. Omoya, Y. Yamamoto, N. Kondo, Optimized gene synthesis and high expression of human interleukin-18, Protein Expr. Purif. 32 (2003) 110–118.
[14] K.E. Griswold, N.A. Mahmood, B.L. Iverson, G. Georgiou, Effects of codon usage versus putative 5′-mRNA structure on the expression of *Fusarium solani* cutinase in the *Escherichia coli* cytoplasm, Protein Expr. Purif. 27 (2003) 134–142.
[15] H. Chen, M. Bjerknes, R. Kumar, E. Jay, Determination of the optimal aligned spacing between the Shine–Dalgarno sequence and the translation initiation codon of *Escherichia coli* mRNAs, Nucleic Acids Res. 22 (1994) 4953–4957.
[16] X. Wu, H. Jornvall, K.D. Berndt, U. Oppermann, Codon optimization reveals critical factors for high level expression of two rare codon genes in *Escherichia coli*: RNA stability and secondary structure but not tRNA abundance, Biochem. Biophys. Res. Commun. 313 (2004) 89–96.
[17] J.T. Chang, C.B. Green, R.E. Wolf Jr., Inhibition of translation initiation on *Escherichia coli* gnd mRNA by formation of a long-range secondary structure involving the ribosome binding site and the internal complementary sequence, J. Bacteriol. 177 (1995) 6560–6567.
[18] C. Brunel, P. Romby, C. Sacerdot, M. de Smit, M. Graffe, J. Dondon, J. van Duin, B. Ehresmann, C. Ehresmann, M. Springer, Stabilised secondary structure at a ribosomal binding site enhances translational repression in *E. coli*, J. Mol. Biol. 253 (1995) 277–290.
[19] C.K. Ma, T. Kolesnikow, J.C. Rayner, E.L. Simons, H. Yim, R.W. Simons, Control of translation by mRNA secondary structure: the importance of the kinetics of structure formation, Mol. Microbiol. 14 (1994) 1033–1047.
[20] C.M. Stenstrom, E. Holmgren, L.A. Isaksson, Cooperative effects by the initiation codon and its flanking regions on translation initiation, Gene 273 (2001) 259–265.
[21] A. Helke, R.M. Geisen, M. Vollmer, M.L. Sprengart, E. Fuchs, An unstructured mRNA region and a 5′ hairpin represent important elements of the *E. coli* translation initiation signal determined by using the bacteriophage T7 gene 1 translation start site, Nucleic Acids Res. 21 (1993) 5705–5711.
[22] C.M. Stenstrom, L.A. Isaksson, Influences on translation initiation and early elongation by the messenger RNA region flanking the initiation codon at the 3′ side, Gene 288 (2002) 1–8.
[23] M. Paulus, M. Haslbeck, M. Watzele, RNA stem–loop enhanced expression of previously non-expressible genes, Nucleic Acids Res. 32 (2004) e78.
[24] M.H. de Smit, J. van Duin, Control of translation by mRNA secondary structure in *Escherichia coli*. A quantitative analysis of literature data, J. Mol. Biol. 244 (1994) 144–150.
[25] B. Klinkert, I. Elles, J. Nickelsen, Translation of chloroplast psbD mRNA in Chlamydomonas is controlled by a secondary RNA structure blocking the AUG start codon, Nucleic Acids Res. 34 (2006) 386–394.
[26] T. Nishikubo, N. Nakagawa, S. Kuramitsu, R. Masui, Improved heterologous gene expression in *Escherichia coli* by optimization of the AT-content of codons immediately downstream of the initiation codon, J. Biotechnol. 120 (2005) 341–346.
[27] J. Pedersen-Lane, G.F. Maley, E. Chu, F. Maley, High-level expression of human thymidylate synthase, Protein Expr. Purif. 10 (1997) 256–262.
[28] E. Lammertyn, L. Van Mellaert, A.P. Bijnens, B. Joris, J. Anne, Codon adjustment to maximise heterologous gene expression in *Streptomyces lividans* can lead to decreased mRNA stability and protein yield, Mol. Gen. Genet. 250 (1996) 223–229.
[29] T.A. Carrier, J.D. Keasling, Controlling messenger RNA stability in bacteria: strategies for engineering gene expression, Biotechnol. Prog. 13 (1997) 699–708.
[30] H. Causton, B. Py, R.S. McLaren, C.F. Higgins, mRNA degradation in *Escherichia coli*: a novel factor which impedes the exoribonucleolytic activity of PNPase at stem–loop structures, Mol. Microbiol. 14 (1994) 731–741.